

# An Enhanced Time Delay Observer for Nonlinear Systems

Suk-Ho Park and Pyung-Hun Chang

**Abstract:** Time delay observer (TDO), thanks to the time delay control (TDC) concept, requires little knowledge of a plant model, and hence is easy to design, robust to parameter variation and computationally efficient, yet can reconstruct states rather reliably for nonlinear plant. In this paper, we propose an improved version of TDO that solves two problems inherent in TDO as follows: TDO displays large reconstruction errors due to low-frequency uncertainty and has some restrictions on selecting its gains. By introducing a low pass filter and a state associated with it, we obtain an enhanced time delay observer (ETDO). This observer turns out to have smaller reconstruction errors than those of TDO and not to have any restriction on selecting its gains, thereby solving the problems. Through performance comparison by transfer function and simulation, we validate the analysis results of two observers (TDO and ETDO) and evaluate the performances. Finally, through experiments on BLDC motor system, the analysis results are clearly confirmed.

**Keywords :** observer, state estimation, time delay observer

## I. Introduction

For nonlinear systems, there are several observer structures that have been reported, which may be summarized as follows: Kalman filter [1] and Luenberger observer [2] for nonlinear systems, global linearization method [3], pseudo-linearization method [4], extended linearization method [5], adaptive scheme observer [6], and sliding mode observer (SMO) [7] [8].

However, the observer structures above require an accurate plant model in their equations inevitably accompanies some practical burdens as follows: without a model, observer cannot be constructed; even if it is available, unless it is accurate enough, a reliable state reconstruction could not be expected; even when a model is accurate enough, the observers could often become too complicated (due to model complexity) to be of practical use, especially on real-time basis [9].

In response to these difficulties, the time delay observer (TDO) was proposed [9]. The essential idea of TDO, which is adopted from the time delay control (TDC) [10], is the use of time-delayed signals to estimate both the plant dynamics and the uncertainties. As the result, TDO requires little knowledge of a plant model, yet can reconstruct states rather reliably for nonlinear plant [9]. Hence, it turns out to be simple to construct, easy to implement due to its efficiency, and robust to parameter variation and disturbance.

For this reason, we believe it worthwhile to enhance it in its performance, which is exactly the purpose of the research in this article. The necessity for such an enhancement came from our observations as follows:

TDO displays large reconstruction errors due to low-frequency uncertainty; and

TDO has some restrictions on selecting its gains: arbitrary pole-placement is not possible.

Therefore, we attempt to report the existence of the problems in TDO, investigate their cause, and propose their remedy in terms of a modified observer structure. More specifically, it will be shown that it is a static filter in TDO that causes the problems; as the remedy, a new observer called

enhanced time delay observer (ETDO) is proposed, by adopting a dynamic low pass filter (LPF) and a state associated with it in place of a static filter. We are going to investigate and prove through analyses and experiments the reconstruction accuracy of ETDO and its no restriction on selecting gains.

The rest of the paper is organized as follows: Section 2 will briefly introduce TDO and investigate its problems. In Section 3, we will propose ETDO, presenting the gain selection method and the stability analysis. In addition, the improvement through ETDO will be analyzed. In Section 4, through comparison by transfer function and simulation, we validate the analysis results and evaluate the performances. In Section 5, through experiments of BLDC motor system, the analysis results are clearly confirmed. Finally, concluding remarks will be drawn in Section 6.

## II. Review of time delay observer

Consider a class of plants that can be expressed in the following SISO nonlinear differential equation:

$$\begin{aligned} \dot{x} &= f(x) + g(x)u + d, \\ y &= x, \end{aligned} \quad (1)$$

where  $\mathbf{x} = [x, \dot{x}, \dots, x^{(n-1)}]^T = [x_1, x_2, \dots, x_n]^T \in \mathcal{R}^n$  denotes the state vector of the system;  $y$  the output;  $u$  the control input;  $f(x)$  the system nonlinearity, which may be unknown;  $g(x)$  the nonlinear control distribution scalar, the range (instead of exact value) of which is known; and  $d$  the unknown disturbance.

Introducing in (1) a constant,  $\hat{g}$ , that represents a value in the known range of  $g(x)$ , we can rearrange (1) into the phase variable form as follows:

$$\begin{aligned} \dot{\mathbf{x}} &= \mathbf{E}_n \mathbf{x} + \mathbf{F}(\mathbf{x}, u) + \hat{\mathbf{G}} \cdot u, \\ y &= \mathbf{C} \mathbf{x}, \end{aligned} \quad (2)$$

where

<sup>1</sup>  $x, y, u, d$  and all other variables derived from these, including the reconstructed states  $\mathbf{z}$ , are functions of time,  $t$ . For instance,  $\mathbf{z} = \mathbf{z}(t)$ .

$$\mathbf{E}_n = \begin{bmatrix} \mathbf{0}_{(n-1) \times 1} & \vdots & \mathbf{I}_{(n-1)} \\ \mathbf{0}_{1 \times n} & & \hat{\mathbf{f}}(\mathbf{x}, u) \end{bmatrix}, \quad \hat{\mathbf{f}}(\mathbf{x}, u) = \begin{bmatrix} \mathbf{0}_{(n-1) \times 1} \\ \hat{f}(\mathbf{x}, u) \end{bmatrix}, \quad (3)$$

$$\hat{\mathbf{G}} = \begin{bmatrix} \mathbf{0}_{(n-1) \times 1} \\ \hat{g} \end{bmatrix}, \quad \mathbf{C} = \begin{bmatrix} 1 & \vdots & \mathbf{0}_{1 \times (n-1)} \end{bmatrix},$$

with  $\mathbf{0}_{i \times j}$  denoting an  $i \times j$  matrix consisting of all zero elements,  $\mathbf{I}_k$  a  $k \times k$  identity matrix, and  $\hat{f}(\mathbf{x}, u)$  the total system uncertainty including the system uncertainty and disturbance, which is expressed as

$$\hat{f}(\mathbf{x}, u) = [f(\mathbf{x}) + g(\mathbf{x}) \cdot u + d] - \hat{g} \cdot u. \quad (4)$$

Note that the system of (2) is globally observable [3].

### 1. Structure of time delay observer

For the analysis of TDO, we will first summarize TDO briefly, and then analyze it. More detailed expositions will be found in [9]. Suppose that for the system of (2), an observer of the following form is available:

$$\dot{\mathbf{z}} = \mathbf{E}_n \mathbf{z} + \hat{\mathbf{f}}(\mathbf{x}, u) + \hat{\mathbf{G}} \cdot u - \mathbf{K} \cdot (z_1 - x), \quad (5)$$

where  $\mathbf{z} = [z_1, z_2, \dots, z_n]^T \in \mathfrak{R}^n$  denotes the reconstructed state vector and  $\mathbf{K} = [K_1, K_2, \dots, K_n]^T \in \mathfrak{R}^n$  the observer gain vector. In order to realize this observer,  $\hat{\mathbf{f}}(\mathbf{x}, u)$  in (5) or  $\hat{f}(\mathbf{x}, u)$  in (4) should be estimated. To this end, instead of using a plant model, TDO uses time delay estimation (TDE) for the estimation of  $\hat{f}(\mathbf{x}, u)$ . In doing so, TDO uses the following assumptions:  $\hat{f}(\mathbf{x}, u)$  is mostly a continuous function or a piece-wise continuous function; and the convergence speed of reconstruction error dynamics can be made much faster than that of the dynamics of  $\hat{f}(\mathbf{x}, u)$ . Then, for a sufficiently small time delay  $L$ , the following estimation is obtained for the total effect of uncertainties,

$$\hat{f}(\mathbf{x}, u) \approx \dot{x}_n - \hat{g} \cdot u \approx \hat{f}(\mathbf{x}_{-L}, u_{-L}) \approx \hat{f}(\mathbf{z}_{-L}, u_{-L}) = \dot{z}_{n-L} - \hat{g} \cdot u_{-L}, \quad (6)$$

where  $\hat{f}(\mathbf{x}_{-L})$  denotes  $\hat{f}(\mathbf{x})|_{t-L}$ .

Substituting (6) into (5) and introducing a static filter lead to the TDO equation as the following:

$$\dot{\mathbf{z}} = \mathbf{E}_n \mathbf{z} + \mathbf{a} \cdot \begin{bmatrix} \mathbf{0}_{1 \times (n-1)} \\ \dot{z}_{n-L} - \hat{g} \cdot u_{-L} \end{bmatrix} + \hat{\mathbf{G}} \cdot u - \mathbf{K} \cdot (z_1 - x), \quad (7)$$

where  $\mathbf{a}$  denotes the constant of static filter. It is noteworthy that TDO uses the static-filtered value of TDE.

### 2. Problems of TDO to be remedied

Without loss of generality, the aforementioned points to be improved can be easily and transparently observed in a 2<sup>nd</sup>-order system. The TDO (7) for the 2<sup>nd</sup>-order system is derived as

$$\begin{aligned} \dot{z}_1 &= z_2 - K_1(z_1 - x), \\ \dot{z}_2 &= \mathbf{a} \cdot [\dot{z}_{2-L} - \hat{g} \cdot u_{-L}] + \hat{g} \cdot u - K_2(z_1 - x). \end{aligned} \quad (8)$$

Based on (11) in [9], the error dynamics can be obtained as

$$\begin{aligned} \dot{e}_1 &= -K_1 e_1 + e_2, \\ \dot{e}_2 &= e_3, \\ \dot{e}_3 &= -\frac{K_2}{aL} e_1 - \frac{(1-a)}{aL} e_3 + y_{ido}, \end{aligned} \quad (9)$$

where  $e_i = z_i - x_i$ ,  $e_3 = \dot{e}_2$ ,

$$y_{ido} = -\frac{K_1 - a}{aL} \hat{f}(\mathbf{x}, u) + \frac{d}{dt} \hat{f}(\mathbf{x}, u) + 2OL \hat{f}(\mathbf{x}, u), \quad (10)$$

with  $OL$  denoting the error with the order of  $L$  due to numerical differentiation and 'ido' in  $(\cdot)_{ido}$  denoting the terms related to TDO.

From the above error dynamics (9), the transfer functions between the errors  $e_1, e_2$  and  $\hat{f}(\mathbf{x}, u)$  can be derived as

$$\frac{e_1(s)}{\hat{f}(s)} = -\frac{s + \frac{1-a}{aL}}{s^3 + \left[ \frac{1-a}{aL} + K_1 \right] s^2 + \frac{1-a}{aL} K_1 s + \frac{K_2}{aL}}, \quad (11)$$

$$\frac{e_2(s)}{\hat{f}(s)} = -\frac{s^2 + \left[ \frac{1-a}{aL} + K_1 \right] s + \frac{1-a}{aL} K_1}{s^3 + \left[ \frac{1-a}{aL} + K_1 \right] s^2 + \frac{1-a}{aL} K_1 s + \frac{K_2}{aL}}. \quad (12)$$

From (11) and (12), therefore, the characteristic equation of the error dynamics (9) is given as follows:

$$s^3 + \left[ \frac{1-a}{aL} + K_1 \right] s^2 + \frac{1-a}{aL} K_1 s + \frac{K_2}{aL} = 0. \quad (13)$$

Since any  $a \geq 1$  makes at least one of the poles of (13) outside the left-half plane,  $a$  should be selected as  $0 < a < 1$  for the stability of (13).

### 2.1 Reconstruction error due to low-frequency uncertainty

Since the transfer functions (11) and (12) behave as low pass filters, the reconstruction errors ( $e_1, e_2$ ) are mainly determined by low-pass-filtered value of the uncertainty  $\hat{f}(\mathbf{x}, u)$ . That is, given the desired observation pole  $\mathbf{I}_d$  (dominant pole in the error dynamics of the observer),  $\hat{f}(\mathbf{x}, u)$  in the low-frequency range,  $0 < \omega \ll \mathbf{I}_d$ , directly affects the reconstruction error, whereas it can be well attenuated in  $\omega \gg \mathbf{I}_d$ .

More specifically, the errors in  $0 < \omega \ll \mathbf{I}_d$ , can be approximated as

$$e_1(s) \approx -\frac{1}{K_2} (1-a) \hat{f}(\mathbf{x}, u) \quad \text{and} \quad e_2(s) \approx -\frac{K_1}{K_2} (1-a) \hat{f}(\mathbf{x}, u).$$

In addition, if the uncertainty  $\hat{f}(\mathbf{x}, u)$  converges to a constant  $\hat{f}(\mathbf{x}_{ss}, u_{ss})$ , the steady-state errors of TDO are calculated to be

$$e_{1,ss} = -\frac{1}{K_2} (1-a) \hat{f}(\mathbf{x}_{ss}, u_{ss}) \quad \text{and} \quad e_{2,ss} = -\frac{K_1}{K_2} (1-a) \hat{f}(\mathbf{x}_{ss}, u_{ss}), \quad (14)$$

which is a finite nonzero value.

### 2.2 Restriction on gain selection

Suppose pole-placement at  $-\mathbf{I}_1, -\mathbf{I}_2$ , and  $-\mathbf{I}_3$  is required to select gains. Comparing, term by term, the coefficients of the characteristic equation (13) with the desired error dynamics,

$$s^3 + (\mathbf{I}_1 + \mathbf{I}_2 + \mathbf{I}_3) s^2 + \mathbf{I}_1 \mathbf{I}_2 + \mathbf{I}_2 \mathbf{I}_3 + \mathbf{I}_3 \mathbf{I}_1 s + \mathbf{I}_1 \mathbf{I}_2 \mathbf{I}_3 = 0,$$

we obtain three algebraic equations as follows:

$$\frac{1-a}{aL} + K_1 = \mathbf{I}_1 + \mathbf{I}_2 + \mathbf{I}_3, \quad (15)$$

$$\frac{1-a}{aL} \cdot K_1 = \mathbf{I}_1 \mathbf{I}_2 + \mathbf{I}_2 \mathbf{I}_3 + \mathbf{I}_3 \mathbf{I}_1, \quad (16)$$

$$\frac{K_2}{aL} = I_1 I_2 I_3, \quad (17)$$

From (15) and (16), in order for  $\|1-a\|/aL$  and  $K_1$  to have real values, the following condition should be met:

$$\|I_1 + I_2 + I_3\|^2 - 4\|I_1 I_2 + I_2 I_3 + I_3 I_1\| \geq 0. \quad (18)$$

Therefore, it can be easily shown that arbitrary pole-placement is not allowed.

A close inspection of (6) and (7) reveals that the low-frequency error problem is a direct outcome of the static filter. While  $a$  less than unity is necessary for stability, it attenuates the TDE,  $\|\dot{z}_{n-L} - \hat{g} \cdot u_{-L}\|$ , by the same ratio of  $a$  throughout the entire frequency range, making the TDE insufficient to cancel out the  $\hat{f}(\mathbf{x}, u)$  in the low-frequency range.

As a direction to resolve the low-frequency observation error problem, we consider a dynamic filter in place of the static filter. Furthermore, the use of a dynamic filter also changes the equation form of (13), the direct cause for the pole-placement problem, thereby resolving the problem as will be shown in Section 3.

### III. Enhanced time delay observer

We propose an observer structure, called ETDO, that adopts a dynamic filter. From its error dynamics, the stability of ETDO is analyzed and its gain selection method is presented. Finally, it will be shown that ETDO indeed provides the remedies to the problems.

#### 1. Structure of enhanced time delay observer

Consider a version of TDO that adopts a first-order low pass filter (LPF) and term it ETDO, which has the structure as follows:

$$\begin{aligned} \dot{\mathbf{z}} &= \mathbf{E}_n \mathbf{z} + [\mathbf{0}_{1 \times (n-1)}; \mathbf{w}]^T + \hat{\mathbf{G}} \cdot u - \mathbf{K} \cdot [z_1 - x], \\ \dot{w} &= -a \cdot w + a[\dot{z}_{n-L} - \hat{g} \cdot u_{-L}], \end{aligned} \quad (19)$$

where  $a$  denotes the cut-off frequency of the LPF and  $w$  the state associated with it. Clearly, ETDO uses the low-pass-filtered value of TDE  $\|\dot{z}_{n-L} - \hat{g} \cdot u_{-L}\|$ , thereby achieving a selective attenuation of TDE only in the high-frequency range.

The error dynamics due to ETDO can be derived from (2) and (19):

$$\dot{\mathbf{e}}_{ot} = \mathbf{A}_{ot} \mathbf{e}_{ot} + \Psi_{etdo}, \quad (20)$$

where  $e_i = z_i - x_i$ ,  $\mathbf{e}_{ot} = [e_1, e_2, \dots, e_n, e_{n+1}]^T \in \mathfrak{R}^{n+1}$ ,  $e_{n+1} = \dot{e}_n$ ,

$$\mathbf{A}_{ot} = \begin{bmatrix} -K_1 & 1 & 0 & \dots & \dots & 0 \\ -K_2 & 0 & 1 & 0 & \dots & 0 \\ \vdots & \vdots & \ddots & \ddots & \ddots & \vdots \\ -K_{n-1} & 0 & \dots & 0 & 1 & 0 \\ 0 & 0 & 0 & \dots & 0 & 1 \\ -\frac{a+K_1 K_2}{1+aL} & -\frac{K_2}{1+aL} & 0 & 0 & \dots & 0 \end{bmatrix}, \quad (21)$$

$$\Psi_{etdo} = [\mathbf{0}_{n \times 1}; \mathcal{Y}_{etdo}]^T, \mathcal{Y}_{etdo} = -\frac{d}{dt} \|\hat{f}(\mathbf{x}, u)\| + \frac{2aL}{1+aL} \|\dot{L}\|, \quad (22)$$

with 'etdo' in  $(\cdot)_{etdo}$  denoting the terms related to ETDO.

The derivation of error dynamics (20) is presented in the

<sup>2</sup> Note that  $\hat{f}(\mathbf{x}, u)$  consists of the system nonlinearity and the disturbance. Thus, the selection of  $L$  needs to be based on the higher bandwidth between those of  $\hat{f}(\mathbf{x}, u)$  and  $d$ .

#### Appendix A.

From (20), one can easily derive the characteristic equation as,

$$s^{n+1} + K_1 s^n + K_2 s^{n-1} + \dots + K_n s^2 + \frac{K_n}{1+aL} s + \frac{aK_n}{1+aL} = 0. \quad (23)$$

Therefore, the gains of ETDO can be chosen from the following procedure:

select a sufficiently small sampling time  $\|L\|$  considering CPU power; and

compare, term by term, the characteristic equation (23) with desired error dynamics and select the gains  $\|K_1, K_2, \dots, K_n$  and  $a\|$  of ETDO.

#### 2. Stability of ETDO

The Lyapunov function based stability analysis of ETDO can be proved in Theorem 1.

**Theorem 1 [Convergence of ETDO]:** In the error dynamics (20), if<sup>3</sup>

$$\text{for all } t > 0, \quad 0 < c_0 < \dots \quad \text{and } 0 < c_1 < \dots,$$

$$\left\| \frac{d}{dt} \|\hat{f}(\mathbf{x}, u)\| \right\| < c_0, \quad \left\| \frac{2aL}{1+aL} \|\dot{L}\| \right\| < c_1, \quad (24)$$

every eigenvalue of  $\mathbf{A}_{ot}$  has a negative real part, be it real or complex,

then the error is exponentially convergent to an open domain,

$$B\|\mathbf{e}_{ot}\| = \|\mathbf{e}_{ot}\| \leq d\mathcal{S}, \quad (25)$$

where  $d = 2 \frac{I_M \|\mathbf{P}\|}{I_m \|\mathbf{Q}\|} \|\Psi_{etdo}\| = 2 \frac{I_M \|\mathbf{P}\|}{I_m \|\mathbf{Q}\|} \|c_0 + c_1\|$  with

$\mathbf{A}_{ot}^T \mathbf{P} + \mathbf{P} \mathbf{A}_{ot} = -\mathbf{Q}$ ; and  $I_M \|\cdot\|$  denoting the maximum eigenvalue and  $I_m \|\cdot\|$  the minimum one.

**Proof:** Defining a Lyapunov function as  $V = \mathbf{e}_{ot}^T \mathbf{P} \mathbf{e}_{ot}$ , one can easily obtain  $\dot{V}$  as follows:

$$\begin{aligned} \dot{V} &= -\mathbf{e}_{ot}^T \mathbf{Q} \mathbf{e}_{ot} + 2\mathbf{e}_{ot}^T \mathbf{P} \Psi_{etdo}, \\ &\leq -I_m \|\mathbf{Q}\| \cdot \|\mathbf{e}_{ot}\|^2 + 2I_M \|\mathbf{P}\| \cdot \|\Psi_{etdo}\| \cdot \|\mathbf{e}_{ot}\|. \end{aligned}$$

Hence, for any  $\|\mathbf{e}_{ot}\|$  that satisfies

$$\|\mathbf{e}_{ot}\| > 2 \frac{I_M \|\mathbf{P}\|}{I_m \|\mathbf{Q}\|} \|\Psi_{etdo}\| = 2 \frac{I_M \|\mathbf{P}\|}{I_m \|\mathbf{Q}\|} \|c_0 + c_1\| = d,$$

$\dot{V}$  remains negative. Therefore, the reconstruction error is exponentially convergent to an open domain,

$$B\|\mathbf{e}_{ot}\| = \|\mathbf{e}_{ot}\| \leq d\mathcal{S}. \quad \blacksquare$$

#### 3. Improvement through ETDO

For the sake of transparent comparison with TDO, 2<sup>nd</sup> order system is considered again, for which ETDO can be derived as

$$\begin{aligned} \dot{z}_1 &= z_2 - K_1 [z_1 - x], \\ \dot{z}_2 &= w + \hat{g} \cdot u - K_2 [z_1 - x], \\ \dot{w} &= -a \cdot w + a[\dot{z}_{2-L} - \hat{g} \cdot u_{-L}]. \end{aligned} \quad (26)$$

From (20), the error dynamics of ETDO can be expressed as

<sup>3</sup> These assumptions are also used in the stability proof of TDO (Chang *et al.*, 1997).

$$\begin{aligned} \dot{e}_1 &= -K_1 e_1 + e_2, \\ \dot{e}_2 &= e_3, \\ \dot{e}_3 &= \frac{1-a+K_1 K_2}{1+aL} e_1 - \frac{K_2}{1+aL} e_2 + \mathbf{y}_{endo}, \end{aligned} \quad (27)$$

and thus the transfer functions between  $e_1, e_2$  and  $\hat{f}[\mathbf{x}, u]$  can be derived as

$$\frac{e_1[s]}{\hat{f}[s]} = -\frac{s}{s^3 + K_1 s^2 + \frac{1}{1+aL} K_2 s + \frac{a}{1+aL} K_2}, \quad (28)$$

$$\frac{e_2[s]}{\hat{f}[s]} = -\frac{s^2 + K_1 s}{s^3 + K_1 s^2 + \frac{1}{1+aL} K_2 s + \frac{a}{1+aL} K_2}. \quad (29)$$

### 3.1 Reconstruction accuracy for low-frequency uncertainty

(28) and (29) show that the reconstruction errors are affected by the band-pass-filtered value of  $\hat{f}[\mathbf{x}, u]$ . Given  $I_d$ , the effect of  $\hat{f}[\mathbf{x}, u]$  can be well attenuated for both  $0 < \mathbf{w} \ll I_d$  and  $\mathbf{w} \gg I_d$ . In addition, the steady-state errors of ETDO become zero for  $\hat{f}[\mathbf{x}, u]$  that converges to a constant. ETDO provides a remedy for the low-frequency error problem associated with TDO. Clearly, the remedy comes from the use of the LPF, which attenuates the TDE only in the high-frequency region.

### 3.2 Free from restriction on gain selection

In ETDO, owing to the different form of its characteristic equation, an arbitrary pole-placement is now possible for the desired error dynamics. More specifically, from (28) and (29), the characteristic equation of the error dynamics of ETDO is given as follows:

$$s^3 + K_1 s^2 + \frac{1}{1+aL} K_2 s + \frac{a}{1+aL} K_2 = 0. \quad (30)$$

Compare term by term the coefficients of the characteristic equation (30) with the error dynamics having arbitrary desired poles ( $-I_1, -I_2$ , and  $-I_3$ ). Then one can obtain three algebraic equations,

$$K_1 = I_1 + I_2 + I_3, \quad (31)$$

$$\frac{1}{1+aL} K_2 = I_1 I_2 + I_2 I_3 + I_3 I_1, \quad (32)$$

$$\frac{a}{1+aL} K_2 = I_1 I_2 I_3. \quad (33)$$

Given  $L$  and the desired poles  $-I_1, -I_2$ , and  $-I_3$ , (31), (32), and (33) enable to select the gains  $K_1, K_2$ , and  $a$  of ETDO without any restriction.

## IV. Performance comparison

For performance comparison, TDO and ETDO for 2<sup>nd</sup>-order system are considered again. By performance we mean paper the reconstruction accuracy and noise rejection ability. If the output  $y$  is corrupted by measurement noise  $\mathbf{u}$ , from (9) and (27), the error dynamics of TDO is obtained as

$$\begin{aligned} \dot{e}_1 &= -K_1 e_1 + e_2 + K_1 \mathbf{u}, \\ \dot{e}_2 &= e_3, \\ \dot{e}_3 &= -\frac{K_2}{aL} e_1 - \frac{1-a}{aL} e_3 + \frac{K_2}{aL} \mathbf{u} + \mathbf{y}_{ido}, \end{aligned} \quad (34)$$

and that of ETDO as

$$\begin{aligned} \dot{e}_1 &= -K_1 e_1 + e_2 + K_1 \mathbf{u}, \\ \dot{e}_2 &= e_3, \\ \dot{e}_3 &= \frac{1-a+K_1 K_2}{1+aL} e_1 - \frac{K_2}{1+aL} e_2 \\ &\quad + \frac{K_2}{1+aL} \dot{\mathbf{u}} - \frac{1-a+K_1 K_2}{1+aL} \mathbf{u} + \mathbf{y}_{endo}, \end{aligned} \quad (35)$$

We are going to compare them in terms of their transfer functions first, and then by simulation.

### 1. Comparison by transfer function

As a significant indication of the performance, the frequency responses of reconstruction accuracy and noise sensitivity can be obtained to evaluate. From (34) and (35), the transfer functions of TDO by Laplace transform are derived as

$$\begin{aligned} e_1[s] &= -\frac{s + \frac{1-a}{aL}}{s^3 + \left[ \frac{1-a}{aL} + K_1 \right] s^2 + \frac{1-a}{aL} K_1 s + \frac{K_2}{aL}} \hat{f}[s] \\ &\quad + \frac{K_1 s^2 + \frac{1-a}{aL} K_1 s + \frac{K_2}{aL}}{s^3 + \left[ \frac{1-a}{aL} + K_1 \right] s^2 + \frac{1-a}{aL} K_1 s + \frac{K_2}{aL}} \mathbf{u}[s], \end{aligned} \quad (36)$$

$$\begin{aligned} e_2[s] &= -\frac{s^2 + \left[ \frac{1-a}{aL} + K_1 \right] s + \frac{1-a}{aL} K_1}{s^3 + \left[ \frac{1-a}{aL} + K_1 \right] s^2 + \frac{1-a}{aL} K_1 s + \frac{K_2}{aL}} \hat{f}[s] \\ &\quad + \frac{\frac{K_2}{aL} s}{s^3 + \left[ \frac{1-a}{aL} + K_1 \right] s^2 + \frac{1-a}{aL} K_1 s + \frac{K_2}{aL}} \mathbf{u}[s], \end{aligned} \quad (37)$$

and those of ETDO are also obtained as

$$\begin{aligned} e_1[s] &= -\frac{s}{s^3 + K_1 s^2 + \frac{1}{1+aL} K_2 s + \frac{a}{1+aL} K_2} \hat{f}[s] \\ &\quad + \frac{K_1 s^2 + \frac{1}{1+aL} K_2 s + \frac{a}{1+aL} K_2}{s^3 + K_1 s^2 + \frac{1}{1+aL} K_2 s + \frac{a}{1+aL} K_2} \mathbf{u}[s], \end{aligned} \quad (38)$$

$$\begin{aligned} e_2[s] &= -\frac{s^2 + K_1 s}{s^3 + K_1 s^2 + \frac{1}{1+aL} K_2 s + \frac{a}{1+aL} K_2} \hat{f}[s] \\ &\quad + \frac{\frac{1}{1+aL} K_2 s^2 + \frac{a}{1+aL} K_2 s}{s^3 + K_1 s^2 + \frac{1}{1+aL} K_2 s + \frac{a}{1+aL} K_2} \mathbf{u}[s]. \end{aligned} \quad (39)$$

In (36)~(39), the first term denotes reconstruction accuracy and the second term noise sensitivity.

Useful insights can be obtained by the following two simplifications: First, the frequency range of system uncertainty  $\hat{f}[\mathbf{x}, u]$  may be assumed to be bounded as

$$\text{for } \mathbf{w} > \mathbf{w}_+, F_f(\mathbf{w}) = 0, \quad (40)$$

where  $F_f(\mathbf{w})$  denotes the Fourier transform of  $\hat{f}[\mathbf{x}, u]$  and

$\mathbf{w}_p$  the bandwidth of plant dynamics including disturbance. Noting in (4) that  $\hat{f}[\mathbf{x}, u]$  is a function of  $\mathbf{x}$ ,  $u$ , and  $d$ , one finds the assumption above reasonable. Since the observer dynamics is made much faster than the plant dynamics, we can select the desired observation poles  $\mathbf{I}_d$  as

$$\mathbf{I}_d \gg \mathbf{w}_p \text{ or } \mathbf{I}_d \approx 10 \cdot \mathbf{w}_p. \quad (41)$$

Secondly, the measurement noise,  $\mathbf{u}$ , is considered as a white noise this is,

$$\text{for all } \mathbf{w}, F_f(\mathbf{w}) \neq 0, \quad (42)$$

where  $F_f(\mathbf{w})$  denotes the Fourier transform of  $\mathbf{u}$ . Note that the noise due to encoder resolution in Section 5 is regarded as a white noise.

For the comparison of transfer functions, we first specify the desired poles for each observer to determine its gains, and then obtain the magnitude plots for comparison. For TDO, poles are specified so that they may meet (18).

Fig. 1 shows the magnitude plots of the transfer functions -- the ratios of  $|e_1|$  and  $|e_2|$  to  $|\hat{f}|$  and  $|\mathbf{u}|$  -- for the poles of  $-\mathbf{I}_d, -\mathbf{I}_d, -4 \cdot \mathbf{I}_d$  with  $\mathbf{I}_d = 30 \text{ rad/s}$ . In terms of reconstruction accuracy shown in Fig. 1(a) and Fig. 1(b), ETDO has the better performance in  $\mathbf{w} < \mathbf{w}_p \approx \mathbf{I}_d/10$ ; yet, in terms of noise sensitivity, Fig. 1(c) and Fig. 1(d) show that TDO is the better, especially in the high-frequency region.

In order to make the comparison more significant, we attempt to take both the accuracy and noise sensitivity together into account. To this end, we first equalize the noise sensitivities of the two observers and compare their accuracies. Their noise sensitivities become approximately similar, when the poles of TDO are set to  $-2.5\mathbf{I}_d, -2.5\mathbf{I}_d, -4 \cdot 2.5\mathbf{I}_d$  with  $\mathbf{I}_d = 30 \text{ rad/s}$ , and those of ETDO to  $-\mathbf{I}_d, -\mathbf{I}_d, -\mathbf{I}_d$  with  $\mathbf{I}_d = 30 \text{ rad/s}$ . Fig. 2 also shows the magnitude plots of the transfer functions. From these plots, although ETDO has the similar noise sensitivity with TDO in Fig. 2(c) and Fig. 2(d), ETDO has better reconstruction accuracy in  $\mathbf{w} < \mathbf{w}_p \approx \mathbf{I}_d/10$  than TDO in Fig. 2(a) and Fig. 2(b).

## 2. Comparison by simulation

To validate the comparison results above, the two observers are applied to the following 2<sup>nd</sup>-order nonlinear system,

$$\begin{aligned} \ddot{x} &= -\mathbf{k} \cdot x^3 + u, \\ y &= x + \mathbf{u}, \end{aligned} \quad (43)$$

where  $\mathbf{k}$  denotes a nonlinear spring constant of  $\mathbf{k} = 1.0$  and  $\mathbf{u}$  a white measurement noise with standard deviation 0.001, and the control input  $u$  is selected as a sinusoidal input ( $u = \sin[0.6\pi t]$ ). Recall that TDO (8) and ETDO (26) for 2<sup>nd</sup>-order system were already derived in Section 2.2 and Section 3.3, respectively.

Note that the time delay for the observers is selected as the same value of the sampling time ( $L$ ),  $0.001 \text{ sec}$  and  $\hat{g}$  is set to 0. The observers are tested for the different desired poles which is expected to show the similar noise sensitivity of TDO and ETDO. That is, the desired poles of TDO are chosen as  $-2.5\mathbf{I}_d, -2.5\mathbf{I}_d, -4 \cdot 2.5\mathbf{I}_d$  with  $\mathbf{I}_d = 30 \text{ rad/s}$ , and those of ETDO to  $-\mathbf{I}_d, -\mathbf{I}_d, -\mathbf{I}_d$  with  $\mathbf{I}_d = 30 \text{ rad/s}$ .

The simulation results are shown in Fig. 3 and Fig. 4. In all

the figures, both (a) and (b) show the states (dotted line) together with the reconstructed states (solid line); both (c) and (d) the reconstruction errors, on which our observation is focused. Clearly, ETDO outperforms TDO in terms of accuracy and noise sensitivity, if marginal for the latter. More specifically, the reconstruction errors of TDO are  $|e_1| < 0.0025$  and  $|e_2| < 0.3$ ; whereas those of ETDO  $|e_1| < 0.0015$  and  $|e_2| < 0.1$  (about 60% and 33% of the errors in TDO, respectively).

## V. Experiment

### 1. Experimental setup

To validate the analysis of TDO and ETDO in a real system, the two observers are applied to a BLDC motor system. The experimental setup of which is shown in Fig. 5. Note that the spring connecting the tip of the link to a wall behaves as a nonlinear spring due to its geometric configuration.

For the experiments, a DSP board is used and a sampling time ( $L$ ) for observers is selected as 0.001s. The angular displacement of the BLDC motor is measured with a rotary encoder of 8000 pulses/rev and the measurement noise due to the resolution is regarded as a white noise. Since we are concerned with the accuracy of state reconstruction, open-loop tests are conducted for which a step input ( $u = 0.8 \text{ volt}$ ) is selected.

To provide the reference velocity for the comparison of accuracy, we obtained it by using a sophisticated off-line numerical differentiation scheme: FIR (finite impulse response)-filter in MATLAB and central numerical differentiation.

### 2. Observers design

The BLDC motor system for the experiments can be regarded as a 2<sup>nd</sup>-order nonlinear system described in (1), with its state vector being defined as  $\mathbf{x} = [x_1, x_2]^T = [\mathbf{q}, \dot{\mathbf{q}}]^T$ . In the design of 2<sup>nd</sup>-order TDO (8) and ETDO (26), the time delay for the observers is selected as the sampling time ( $L$ ), 0.001s and  $\hat{g}$  is set to 0. The gains  $(K_1, K_2, \mathbf{a})$  for TDO and  $(K_1, K_2, \mathbf{a})$  for ETDO are selected for the following poles: for TDO,  $-2.5\mathbf{I}_d, -2.5\mathbf{I}_d, -4 \cdot 2.5\mathbf{I}_d$ , (with  $\mathbf{I}_d = 30 \text{ rad/s}$ ); for ETDO,  $-\mathbf{I}_d, -\mathbf{I}_d, -\mathbf{I}_d$ , (with  $\mathbf{I}_d = 30 \text{ rad/s}$ ).

### 3. Observation results

Fig. 6 and Fig. 7 show the experimental results of TDO and ETDO, respectively. In these figures, both (a) and (b) show the states (dotted line) together with the reconstructed states (solid line); both (c) and (d) the reconstruction errors, which are plotted again in different scales in Fig. 8 for a close inspection.

The results show that ETDO generally outperforms TDO in terms of both accuracy and noise sensitivity. Fig. 8 reveals that the major portion of the error of TDO is accounted for by a low-frequency component apparently caused by its static filter. At the same time, the error of ETDO in Fig. 8 portrays how the LPF in ETDO is reducing the low-frequency error due to TDO, thereby demonstrating its effectiveness. To summarize, the experimental results confirm the analysis results of TDO and ETDO.

## VI. Conclusion

In this paper, we have analyzed TDO and have reported its problems as follows:

TDO displays large reconstruction errors due to low-frequency uncertainty; and

TDO has some restrictions on selecting its gains: arbitrary pole-placement is not possible.

To remedy these problems, we have proposed ETDO using a LPF instead of the static filter in TDO. In addition, the error dynamics of ETDO and the procedure of gain selection have been presented. As a result, ETDO has smaller reconstruction errors than TDO and no restriction on gain selection. Through the performance comparisons and the experiments of BLDC motor system, we could verify the analysis results of TDO and ETDO. Consequently, ETDO has been shown to not only remedy the problems of TDO, but also preserve the positive attributes of TDO.

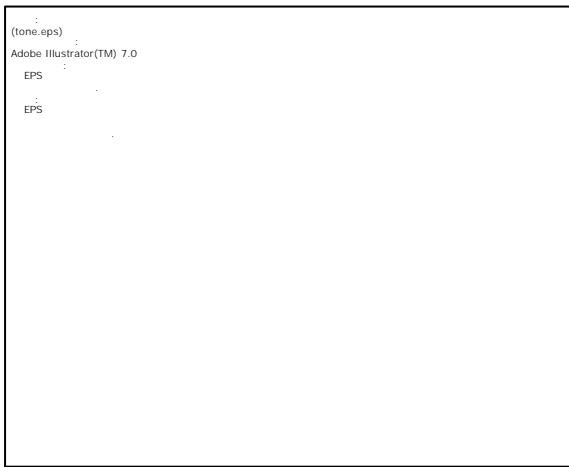


Fig. 1. Magnitude plot of TDO (thin line) and ETDO (solid line) -- the ratios of  $|e_1|$  and  $|e_2|$  to  $|\hat{f}|$  and  $|\mathbf{u}|$  -- with the same desired poles  $(-I_d, -I_d, -4 \cdot I_d$  with  $I_d = 30rad/s)$ .



Fig. 2. Magnitude plot of TDO (thin line) and ETDO (solid

line) -- the ratios of  $|e_1|$  and  $|e_2|$  to  $|\hat{f}|$  and  $|\mathbf{u}|$  -- with the different desired poles (TDO :  $-2.5I_d, -2.5I_d, -4 \cdot 2.5I_d$  and ETDO:  $-I_d, -I_d, -I_d$  with  $I_d = 30rad/s)$ .

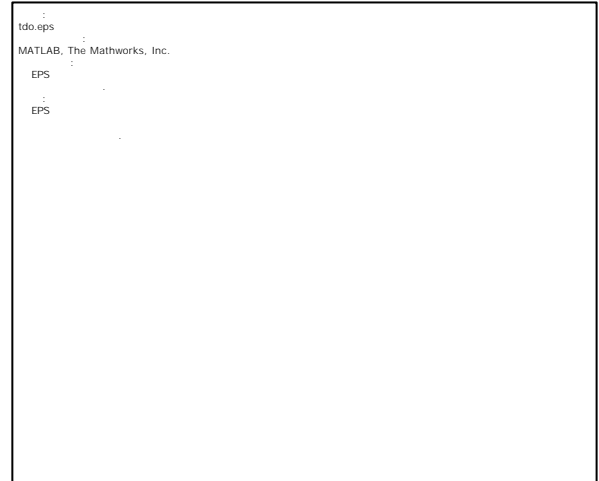


Fig. 3. Simulation results of TDO: Both (a) and (b) show the states (dotted line) together with the reconstructed states (solid line); both (c) and (d) the reconstruction errors.

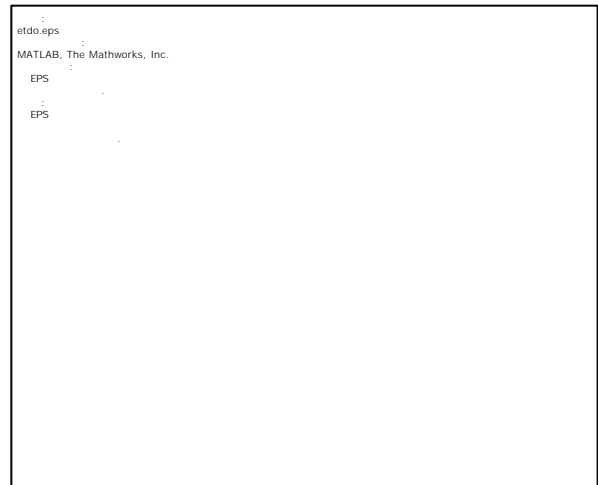


Fig. 4. Simulation results of ETDO: Both (a) and (b) show the states (dotted line) together with the reconstructed states (solid line); both (c) and (d) the reconstruction errors.

<sup>4</sup> When  $L$  is set less than 0.001 s, the reconstruction errors tend to decrease, yet the improvement is not noticeable; when  $L$  becomes larger than 0.001 s, the errors increase. However, excessive large  $L$  makes the observer unstable.

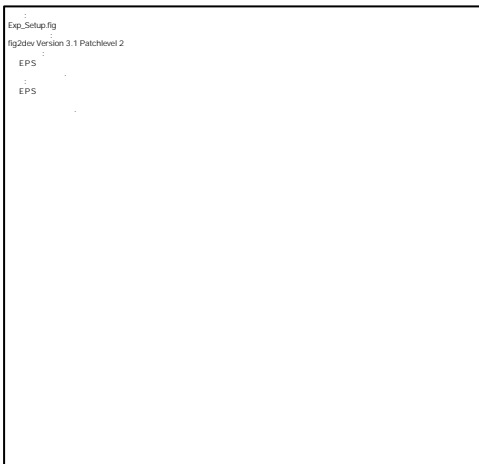


Fig. 5. Experimental setup: BLDC motor system with the spring connecting the tip of the link to a wall.

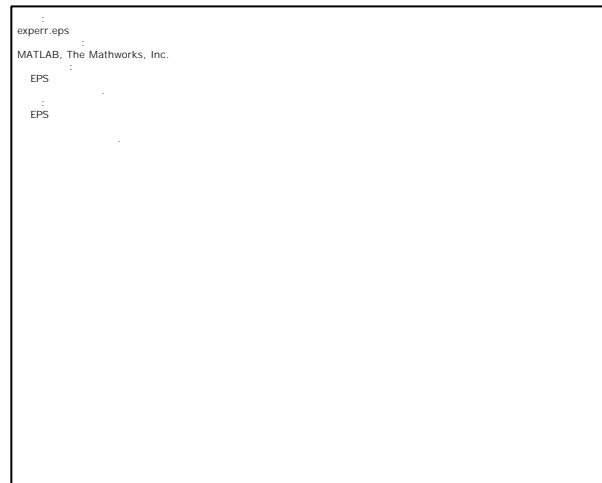


Fig. 8. Reconstruction error of TDO and ETDO: Both (a) and (b) show the reconstruction errors of TO (dotted line) and ETDO (solid line).

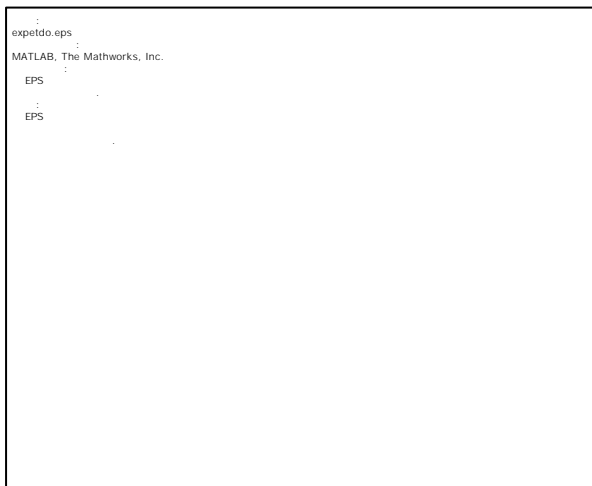


Fig. 6. Experimental results of TDO: Both (a) and (b) show the states (dotted line) together with the reconstructed states (solid line); both (c) and (d) the reconstruction errors.

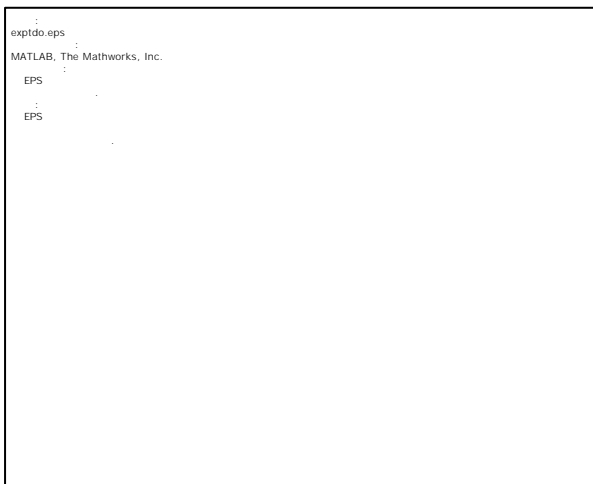


Fig. 7. Experimental results of ETDO: Both (a) and (b) show the states (dotted line) together with the reconstructed states (solid line); both (c) and (d) the reconstruction errors.

### Reference

- [1] R. E. Kalman, "On a new approach to filtering and prediction problems," *ASME J. Basic Engineering*, vol. 28, 1960.
- [2] D. G. Luenberger, "Observers for multivariable systems," *IEEE. Trans. Automatic Control*, vol. 11, pp. 190-197, 1966.
- [3] M. Zeitz, "Observability canonical (Phase-Variable) form for nonlinear time-variable systems," *Int. J. Systems Science*, vol. 15, pp. 949-958, 1984.
- [4] P. Tomei, "An observer for flexible robots," *IEEE. Trans. Automatic Control*, vol. 5, pp. 739-743, 1990.
- [5] W. T. Baumann and W. J. Rugh, "A stable adaptive observer for a class of nonlinear second-order systems," *Analysis and Optimization of Systems*, pp. 143-155, 1986.
- [6] M. Gevers and G. Bastin, "A stable adaptive observer for a class of nonlinear second-order systems," *Analysis and Optimization of Systems*, pp. 143-155, 1986.
- [7] J. -J. E. Slotine, J. K. Hedrick, and E. A. Misawa, "On sliding observers for nonlinear systems," *ASME J. Dynamic Systems, Measurement and Control*, vol. 109, pp. 245-252, 1987.
- [8] C. Canudas de Wit and J. -J. E. Slotine, "Sliding observers for robot manipulators," *Automatica*, vol. 27, pp. 859-864, 1991.
- [9] P. H. Chang, J. W. Lee, J. W., and S. H. Park, "Time delay observer: A robust observer for nonlinear plants," *ASME J. Dynamic Systems Measurement and Control*, vol. 119, pp. 521-527, 1997.
- [10] K. Youcef-Toumi and O. Ito, "A time delay controller design for systems with unknown dynamics," *ASME J. Dynamic Systems Measurement and Control*, vol. 112, pp. 133-142, 1990.

### Appendix

#### A. Derivation of error dynamics in ETDO

Except the last two equations in the error dynamics (20), the

remaining error dynamics can be straightforwardly derived from (2) and (19). Then, in this appendix, the last two equations in (20) are derived.

From (2) and (19), the error dynamics of  $(e_n)$  can be derived as

$$\dot{e}_n = -K_n e_1 + w - \hat{f}. \tag{44}$$

Defining  $e_{n+1} = \dot{e}_n$ , its derivative becomes

$$\dot{e}_{n+1} = -K_n \dot{e}_1 + \dot{w} - \frac{d}{dt}(\hat{f}), \tag{45}$$

where  $\dot{e}_1$ , from the first equation in (20), can be rewritten as

$$\dot{e}_1 = -K_1 e_1 + e_2. \tag{46}$$

Besides, the derivative of  $w$  in (19) can be expressed as

$$\begin{aligned} \dot{w} &= -a \cdot w + a \cdot \begin{bmatrix} \dot{z}_{n-L} - \hat{g} \cdot u_{-L} \\ \dot{z}_{n-L} - \dot{x}_{n-L} + \dot{x}_{n-L} - \hat{g} \cdot u_{-L} \end{bmatrix}, \\ &= -a \cdot w + a \cdot \begin{bmatrix} \dot{z}_{n-L} - \dot{x}_{n-L} + \dot{x}_{n-L} - \hat{g} \cdot u_{-L} \\ \dot{e}_{n-L} - \hat{f}_{-L} \end{bmatrix}, \end{aligned} \tag{47}$$

where  $\dot{e}_{n-L} = \dot{z}_{n-L} - \dot{x}_{n-L}$  and  $\hat{f}_{-L} = \dot{x}_{n-L} - \hat{g} \cdot u_{-L}$  from  $\hat{f} = \dot{x}_n - \hat{g} \cdot u$  of (6).

Combining (44), (46) and (47) with (45),

$$\begin{aligned} \dot{e}_{n+1} &= -K_n \begin{bmatrix} -K_1 e_1 + e_2 \\ -a \cdot \begin{bmatrix} \dot{z}_{n-L} - \dot{x}_{n-L} + \dot{x}_{n-L} - \hat{g} \cdot u_{-L} \\ \dot{e}_{n-L} - \hat{f}_{-L} \end{bmatrix} + a \cdot \begin{bmatrix} \dot{e}_{n-L} - \hat{f}_{-L} \\ \dot{e}_{n-L} - \hat{f}_{-L} \end{bmatrix} - \frac{d}{dt}(\hat{f}) \end{bmatrix}, \\ &= \begin{bmatrix} -a + K_1 \\ K_n e_1 - K_n e_2 - a \cdot \begin{bmatrix} \dot{z}_{n-L} - \dot{x}_{n-L} + \dot{x}_{n-L} - \hat{g} \cdot u_{-L} \\ \dot{e}_{n-L} - \hat{f}_{-L} \end{bmatrix} - \frac{d}{dt}(\hat{f}) \end{bmatrix}, \\ &= \begin{bmatrix} -a + K_1 \\ K_n e_1 - K_n e_2 - aL \cdot \begin{bmatrix} \dot{e}_{n+1} \\ \dot{e}_{n+1} \end{bmatrix} - aL \cdot \begin{bmatrix} \frac{d}{dt}(\hat{f}) \\ \frac{d}{dt}(\hat{f}) \end{bmatrix} + aL \cdot \begin{bmatrix} \frac{d}{dt}(\hat{f}) \\ \frac{d}{dt}(\hat{f}) \end{bmatrix} \end{bmatrix} \end{aligned}$$

Finally, from the above equation, the derivative of  $e_{n+1}$  results as follows:

$$\dot{e}_{n+1} = \begin{bmatrix} -a + K_1 \\ K_n \end{bmatrix} \begin{bmatrix} e_1 \\ e_2 \end{bmatrix} - \frac{2aL}{1+aL} \begin{bmatrix} \frac{d}{dt}(\hat{f}) \\ \frac{d}{dt}(\hat{f}) \end{bmatrix} - \frac{2aL}{1+aL} \begin{bmatrix} \frac{d}{dt}(\hat{f}) \\ \frac{d}{dt}(\hat{f}) \end{bmatrix} \tag{48}$$



**Suk-Ho Park**

He received the B.S.P.E. and M.S.M. E. degrees from KAIST, Taejon, Korea, in 1993 and 1995, respectively. Since 1995, he has been at Korea Advanced Institute of Science and Technology (KAIST), where he is a Ph. D. candidate in mechanical engineering. His research interests include the robust observer and control for nonlinear system, control of pneumatic system and robust control application.

His research interests include the robust observer and control for nonlinear system, control of pneumatic system and robust control application.



**Pyung-Hun Chang**

He received the B.S.M.E. and M.S.M. E. degrees from Seoul National University (SNU), Seoul, Korea, in 1974 and 1977, respectively. He received the Ph. D. degree in mechanical engineering from the Massachusetts Institute of Technology (MIT), Cambridge, MA, in 1987. From 1989-1995, he was an Assistant Professor with the Department of Mechanical Engineering, KAIST, Taejon, Korea. Since 1995, he has been an Associate Professor with KAIST. His research interests include the robust observer and control for nonlinear system, input shaping technique, system modeling, pneumatic system, redundant robots, service robot, and universal robot controller.

His research interests include the robust observer and control for nonlinear system, input shaping technique, system modeling, pneumatic system, redundant robots, service robot, and universal robot controller.



